

Chapter 3

Capillarity



3.1 Curvature of a Phase-Field Contour

In the previous chapter, the meanings of individual terms, the gradient and potential contributions of the free-energy functional [Eqs. (2.7) and (2.8), respectively], and their functional derivatives were discussed. In the free-energy functional, both terms contribute $\frac{1}{2}$ of the interface energy σ . In the phase-field equation of motion, either for the double-well potential (2.28) or double-obstacle potential (2.36), they cancel to 0 in 1D for the correct analytical solution. If the numerical solution deviates from the analytical solution, either because one has started from wrong initial conditions or because of numerical errors, the two terms act to push the interface to the right solution, i.e., they stabilize the interface contour. For a curved interface in 3D, it has already been mentioned that these terms do not cancel! They have the property to evaluate “curvature.” This will be proven in this third chapter.

To summarize: the phase-field equation has two important properties: (i) to propagate the interface with a velocity related to the bulk free-energy difference Δg between different phases such that the energetically lower phase will grow and the other phase will shrink; (ii) to correct this transformation process for “capillarity” related to the local curvature of the interface. The latter also considers interface-energy anisotropy, which is a dominant effect in many metallurgical processes. This will be detailed in the second part of this chapter. Let us first prove the relation between the surface terms in the phase-field equation and curvature.

The formal mathematical definition of the curvature κ of any vector field is the divergence of the normal vector \vec{n} :

$$\kappa = \vec{\nabla} \cdot \vec{n} = \vec{\nabla} \cdot \frac{\vec{\nabla} \phi}{|\vec{\nabla} \phi|}. \quad (3.1)$$

Of course, we evaluate this for our phase field ϕ . Applying the divergence to the numerator and denominator of $\frac{\vec{\nabla}\phi}{|\vec{\nabla}\phi|}$ gives:

$$\begin{aligned} \kappa &= \frac{1}{|\vec{\nabla}\phi|} \nabla^2 \phi - \frac{\vec{\nabla}\phi}{|\vec{\nabla}\phi|^2} \vec{\nabla} \cdot |\vec{\nabla}\phi| \\ &= \frac{1}{|\vec{\nabla}\phi|} \left[\nabla^2 \phi - \frac{\vec{\nabla}\phi}{|\vec{\nabla}\phi|} \vec{\nabla} \cdot |\vec{\nabla}\phi| \right] \end{aligned} \quad (3.2)$$

$$\begin{aligned} &= \frac{1}{|\vec{\nabla}\phi|} \left[\nabla^2 \phi - \vec{n} \cdot \vec{\nabla} \cdot |\vec{\nabla}\phi| \right] \\ &= \frac{1}{|\vec{\nabla}\phi|} \left[\nabla^2 \phi - \frac{\partial^2}{\partial n^2} \phi \right] \end{aligned} \quad (3.3)$$

$$= \frac{1}{|\vec{\nabla}\phi|} \left[\nabla^2 \phi - \frac{\pi^2}{\eta^2} \left(\frac{1}{2} - \phi \right) \right]. \quad (3.4)$$

We have inserted the definition of \vec{n} into Eq. (3.2). This projects the divergence $\vec{\nabla} \cdot |\vec{\nabla}\phi|$ onto the normal through the interface, so this operator can be replaced by the second derivative in the normal direction in Eq. (3.3). We know this second derivative from the 1D analysis, Eqs. (2.18) or (2.32) for the double-well or double-obstacle potentials, respectively. In the last Eq. (3.4), the relation for the double-obstacle potential is inserted. The relation for the double-well potential works analogously. We see that this is exactly the expression used in the previous chapter for the evaluation of the capillarity term in the Gibbs–Thomson equation (cf. Fig. 2.3).

3.2 Anisotropy of Interface Energy

In the previous chapter, dealing with the analytic relation of a phase-field equation and the phenomenological Gibbs–Thomson equation for interface motion including capillarity, all entities—i.e., the phase-field mobility M^ϕ , the interface energy σ , the interface width η , and the thermodynamic driving force Δg —were taken as constants. This is, in general, not the case; sometimes it is a strong oversimplification. The mobility and the interface energy are anisotropic functions of the orientation of the interface with respect to the orientation of the adjacent phases. One distinguishes so-called “inclinations” of the interface with respect to the crystallographic orientation of individual crystal phases, and the misorientation

of these phases if they are crystalline solids. In general, we have to specify three misorientation angles and two inclinations: five angles in total. This poses a challenge for determining these functions, but it also generates challenges for phase-field models in terms of coping with these functions.

The mobility M^ϕ is relatively easy; it is simply a scalar proportionality factor between time t and the so-called kinetic driving force acting on the interface, i.e., the “capillarity-corrected bulk free-energy difference.” It will, in general, vary from point to point in the interface, because the misorientation and inclination angles of a curved interface vary along the interface. Depending on the physical model used for the mobility, it may cause numerical problems regarding time-stepping schemes (because it relates to time). However, from a conceptual point of view, it is easy and does not need further discussion here. In contrast, the interface energy is more difficult.

3.2.1 Interface-Energy Anisotropy: Phenomenological Picture

Interface-energy anisotropy is a conceptual challenge. For phenomenology, we will only discuss the simple case of a crystalline inclusion in an amorphous matrix, say a liquid. Then, the dependence of the interface energy on misorientation (three angles) vanishes. We will only consider two dimensions; then, only one inclination angle θ with respect to the crystal axis θ_0 remains (see Fig. 3.1). The Gibbs–Thomson equation [see Chap. 1, Eq. (1.5)] becomes:

$$\vec{v} = \vec{n}M (\sigma^*\kappa + \Delta g). \quad (3.5)$$

Here, $\sigma^* = \sigma + \sigma''$, with $\sigma'' = \frac{\partial^2}{\partial \theta^2} \sigma$, is called the “interface stiffness,” i.e., the resistivity of the interface to bending. σ'' is also called the “Herring torque,” as it was introduced by Herring in 1952 [3]. This tells us that the interfacial energy of a precipitate can be reduced by two separate mechanisms: (i) that the interface area is reduced; and (ii) that the interface is turned into a low-energy inclination. In fact, for the equilibrium shape of the precipitation surrounded by its melt, the interplay of both mechanisms has significant consequences. Equilibrium here is defined as the chemical potential over the system being constant. Furthermore, the precipitate neither grows nor shrinks, i.e., $\vec{v} = 0$. Since the precipitate has a curved interface, there is a potential jump of $\sigma^*\kappa$ between the bulk energy of the precipitate and the matrix, the so-called “capillarity pressure.”

The Gibbs–Thomson equation (1.5) becomes ($\vec{v} = 0$):

$$\begin{aligned} 0 &= \sigma^*\kappa + \Delta g \\ \sigma^*\kappa &= -\Delta g = \text{constant}. \end{aligned} \quad (3.6)$$

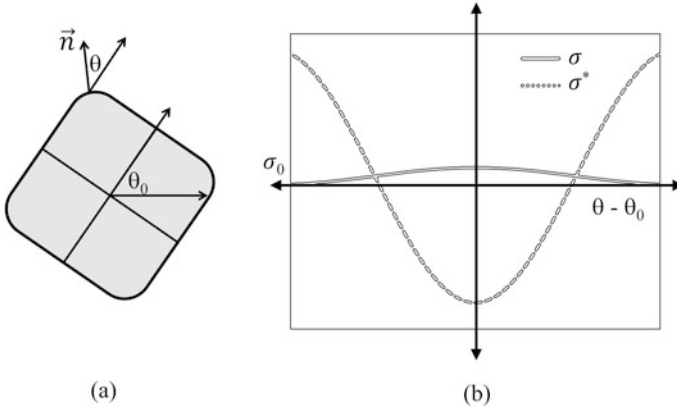


Fig. 3.1 (a) Sketch of the equilibrium shape of a crystal with strong interface anisotropy. The preferred crystallographic axis is rotated by θ_0 from the x axis. The surface normal at one specific point at the rounded corner is tilted by θ from the preferred axis. (b) The interface energy σ and interface stiffness σ^* as functions of $\theta - \theta_0$

If $\sigma^* \kappa = \text{constant}$ all along the interface, then σ^* has to be inversely proportional to κ , or, because σ^* is a material constant, κ has to be inversely proportional to σ^* . Where the stiffness is high, the curvature of the interface has to be low. If the stiffness is low, the interface can be easily bent, and we have edges or corners. We also know that the interface energy is high at edges and corners, so the interface area must be small. As a take-away message: where the interface energy is high, the stiffness is low, and vice versa. All of this is “general physics”, not specific to phase field. It is the classical picture as drawn by Wulff [10], Herring [3], and others. But phase field incorporates this physics naturally. In the phase-field literature about dendritic growth, a simple anisotropy function with fourfold symmetry, in which the strength of the anisotropy is δ , is popular:

$$\sigma(\theta) = \sigma_0(1 + \delta \cos[4(\theta - \theta_0)]) \quad (3.7)$$

$$\begin{aligned} \sigma^*(\theta) &= \sigma_0(1 + \delta \cos 4(\theta - \theta_0) - 16\delta \cos 4(\theta - \theta_0)) \\ &= \sigma_0(1 - 15\delta \cos 4(\theta - \theta_0)). \end{aligned} \quad (3.8)$$

Before ending this section, let us make several remarks:

Firstly, we see that for $\delta > \frac{1}{15}$, the stiffness becomes negative (for $\theta = 0$). Phenomenologically speaking, inclinations of the interface that have a negative stiffness are forbidden. They collapse into edges and corners of the crystal: the crystal surface has “missing angles.” In phase fields, this is not possible to realize, since, due to the diffuseness of the interface, edges and corners are always rounded off with a maximum curvature of the order of the reciprocal interface width $\frac{1}{\eta}$. Therefore, one has to “regularize” the corresponding function of the interface

stiffness with respect to orientation, cutting it to a positive minimum value of the stiffness. We regard this as “technical.”

Secondly, in 3D, i.e., having two inclination angles, one usually expands the interface energy and the stiffness in spherical harmonics. For a strongly anisotropic interface energy, e.g., for faceted crystals, other models may be appropriate (see Example at the end of this chapter).

Thirdly, in a solid, we also need to consider the three misorientation angles for each inclination-angle landscape.

Finally, at the atomistic scale, i.e., for nanocrystals, all these phenomenological relations—and also their microscopic or mesoscopic phase-field equivalents—will break down! The description of “capillarity” by curvature is only a statistical description of the atomic movement at interfaces. Atoms do not care about the curvature that we measure at an interface at a scale large compared to the atomic scale. But collectively they behave as if they would follow these rules. And there are other effects involved in the atomic motion connected to interfaces such as coupled-motion [1] or stress–strain effects at the nanoscale [2, 8]. Figure 3.1a schematically explains the meaning of the inclination angle with respect to the crystallographic axis and the normal vector of the interface in 2D. Figure 3.1b displays a simple model for the interface energy and stiffness as functions of the inclination angle.

3.2.2 Interface-Energy Anisotropy: Phase-Field Picture

In phase-field theory, the whole issue of interface-energy anisotropy is considered naturally, though there currently remain many open issues of technical character: it is not so easy. Let us start from the beginning, the phase-field equation as the functional derivative of the free energy, Eq. (2.6):

$$\frac{\delta\phi}{\delta t} \propto -\frac{\delta F}{\delta\phi}. \quad (3.9)$$

Here, we will only investigate the capillarity contribution, i.e., we will neglect the bulk energy difference between phases $\Delta g = 0$. In the physical notation, with anisotropic interface energy $\sigma(\vec{n})$ as a function of the normal vector to the interface \vec{n} but with isotropic interface width η , the variation of the free energy then becomes:

$$\delta F = \int_{\Omega} d^3x \left\{ \eta\sigma(\vec{n}) \delta \left[(\nabla\phi)^2 + \frac{\pi^2}{\eta^2} |\phi(1-\phi)| \right] \right. \quad (3.10)$$

$$\left. + \eta \delta\sigma(\vec{n}) \left[(\nabla\phi)^2 + \frac{\pi^2}{\eta^2} |\phi(1-\phi)| \right] \right\}. \quad (3.11)$$

We use the double-obstacle potential; the case with the double-well potential works identically. In the first part (3.10), the variation is applied to the gradient

and potential contributions. This part we already know from Chap. 2, Eq. (2.15). The new part is the variational derivative of the interface energy (3.11) since it is anisotropic with respect to inclination, and the interface normal \vec{n} is a function of the gradient of the phase field $\vec{n} = \frac{\vec{\nabla}\phi}{|\vec{\nabla}\phi|}$. First, we notice that the term in the square brackets of Eq. (3.11) is a positive function of ϕ and can be approximated, neglecting higher-order curvature terms and using relation (2.31):

$$\left[(\nabla\phi)^2 + \frac{\pi^2}{\eta^2} |\phi(1-\phi)| \right] \approx 2(\nabla\phi)^2. \quad (3.12)$$

A general discussion of the variation $\delta\sigma(\vec{n})$ in 3D is quite involved, so we restrict ourselves here to 2D for the sake of tractability. Setting the rotation angle to zero $\theta_0 = 0$, we define the angle of the surface normal $\theta = \arctan(\frac{\phi_y}{\phi_x})$ with the derivative of ϕ in the x and y directions of a Cartesian coordinate system. Then we expand:

$$\delta\sigma(\theta) (\nabla\phi)^2 = \frac{\partial\sigma(\theta)}{\partial\theta} \delta\theta (\nabla\phi)^2 \quad (3.13)$$

$$= \frac{\partial\sigma(\theta)}{\partial\theta} \frac{\phi_x \delta\phi_y - \phi_y \delta\phi_x}{(\nabla\phi)^2} (\nabla\phi)^2 \quad (3.14)$$

$$= \frac{\partial\sigma(\theta)}{\partial\theta} (\phi_x \delta\phi_y - \phi_y \delta\phi_x) \quad (3.15)$$

$$= - \left[\frac{\partial}{\partial y} \left(\frac{\partial\sigma(\theta)}{\partial\theta} \phi_x \right) \delta\phi - \frac{\partial}{\partial x} \left(\frac{\partial\sigma(\theta)}{\partial\theta} \phi_y \right) \delta\phi \right]$$

$$= \frac{\partial^2\sigma(\theta)}{\partial\theta^2} \left(\frac{\partial\theta}{\partial y} \phi_x - \frac{\partial\theta}{\partial x} \phi_y \right) \delta\phi$$

$$\approx \frac{\partial^2\sigma(\theta)}{\partial\theta^2} |\nabla\phi| \kappa \delta\phi. \quad (3.16)$$

We leave the proof of this relation as an exercise. To help with this: we have three different differentials to consider in expanding the variation $\delta\sigma(\theta)$. Be reminded that all these differentials are linear operators that commute. In Eq. (3.13), the chain rule is used to expand the variation of σ into a differential in θ and a variation in θ . Then, in Eq. (3.14), the variation in θ is expanded in differentials in ϕ_x and ϕ_y , which by themselves are differentials in space. Then, partial integration is applied to the last term in Eq. (3.15) to respectively integrate the variations $\delta\phi_x$ and $\delta\phi_y$ in space to separate the single variation $\delta\phi$ (again neglecting boundary integral terms). This needs a lot of bookkeeping, but it is more or less straightforward. The final step $\frac{\partial\theta}{\partial y} \phi_x - \frac{\partial\theta}{\partial x} \phi_y \approx |\nabla\phi| \kappa$ is an approximation to lowest order in κ , where the variation of the angle along one Cartesian direction is weighted by the phase-field gradient in the other direction. This variation, clearly, has to vanish for a planar interface where the curvature is 0.

Collecting all contributions, we end up with the desired expression for the evolution of the phase field (valid for $0 < \phi < 1$ and $\Delta g \neq 0$), the equivalent of (2.36):

$$\frac{\partial \phi}{\partial t} = M^\phi \left\{ (\sigma + \sigma'') \left[\nabla^2 \phi - \frac{\pi^2}{\eta^2} \left(\frac{1}{2} - \phi \right) \right] - \frac{\pi}{\eta} \sqrt{\phi(1-\phi)} \Delta g \right\}. \quad (3.17)$$

Please note that throughout Chap. 2, the interface energy σ was taken as isotropic, so no torque σ'' was considered. In general, this should always be there, as interfaces in crystalline phases are always dependent on orientation and inclination, even if only weakly. Several aspects shall be remarked upon. The form of Eq. (3.17) may not be the optimal choice for a numerical solution, since the prefactor $\sigma^* = \sigma + \sigma''$ in front of the Laplacian can be strongly varying for strong anisotropies. If an explicit time-stepping scheme is used for the phase-field equation, this may lead to a significant reduction of the possible time steps and/or it may introduce instabilities in the front. An alternative is to evaluate the curvature of the interface locally and average it within a certain region. Then, one can use the Herring torque term σ'' as a smoothly varying driving force for the interface. Alternatively, one may directly discretize the variation $\delta\sigma(\vec{n})$, Eq. (3.11), as done, e.g., in [4]. A comparison of different approaches for dendritic growth is given in [5].

3.3 Exercises

Exercise

Repeat for yourself the relation of the mathematical curvature (3.1) with the corresponding phase-field expression (3.4). Consider that this relation is only true if the phase field is in the “right contour.”

Exercise

Prove the derivation of the Herring torque from the phase-field functional (3.16).

Example—Equilibrium Shapes

Anisotropy of interface energy is important in materials because it significantly impacts the morphology of the grain surface, the kinetics of interface migration, and the overall structure of the composite. According to the conventional definition of interface-energy anisotropy, it can be described as a function of the crystallographic orientation of the interface, which results in the equilibrium forms of individual crystals given by the Wulff construction [10]. We use an anisotropy model here, with the interface energy being a function of the inclination angle θ only. The interface stiffness with respect to the inclination angle is modeled as [7]:

$$\sigma_{\alpha}^* = \sigma_{\alpha}(\theta_{\alpha}) + \sigma''(\theta_{\alpha}) = \frac{\sigma^0 a^2}{(\sin^2(\theta_{\alpha}) + a^2 \cos^2(\theta_{\alpha}))^{\frac{3}{2}}}. \quad (3.18)$$

Validation of the Equilibrium Shapes

The **proposed model** was employed in a 3D simulation box with 64^3 grid points of an initially spherical grain inserted into the melt. The inclination angle is computed using the interface normal of the phase field and different basic sets of facet normals, as shown in Fig. 3.2.

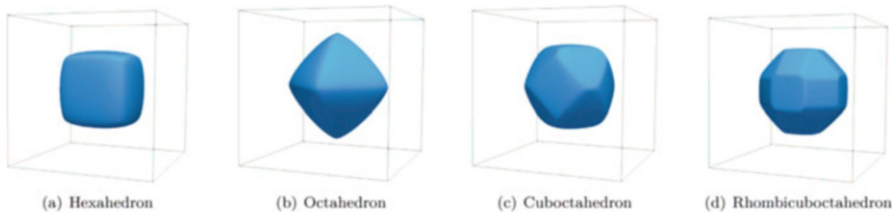


Fig. 3.2 Equilibrium shapes with different facet vectors: (a) only $\{100\}$ facets; (b) only $\{111\}$ facets; (c) $\{100\}$ and $\{111\}$ facets; (d) $\{100\}$, $\{110\}$, and $\{111\}$ facets

Further Reading

- Rigorous derivation of the phase-field Herring torque: [6].
- Cahn–Hoffmann ξ -vector formalism: [9].

References

1. J.W. Cahn, Y. Mishin, A. Suzuki, Coupling grain boundary motion to shear deformation. *Acta Mater.* **54**(19), 4953–4975 (2006). ISSN: 1359-6454. <https://doi.org/10.1016/j.actamat.2006.08.004>. <https://www.sciencedirect.com/science/article/pii/S1359645406005313>.
2. R. Darvishi Kamachali et al., Multiscale simulations on the grain growth process in nanostructured materials. *Int. J. Mater. Res.* **101**, 1332–1338 (2010). <https://doi.org/10.3139/146.110419>
3. C. Herring, The use of classical macroscopic concepts in surface-energy problems, in *Structure and Properties of Solid Surfaces*, ed. by R. Gomer, C.S. Smith. (University of Chicago Press, Chicago, 1952)
4. H.K. Kim et al., Phase-field modeling for 3D grain growth based on a grain boundary energy database. *Model. Simul. Mater. Sci. Eng.* **22**(3), 034004 (2014). <https://doi.org/10.1088/0965-0393/22/3/034004>
5. J. Kundin, I. Steinbach, Comparative study of different anisotropy and potential formulations of phase-field models for dendritic solidification. *Comput. Mater. Sci.* **170**, 109197 (2019). <https://doi.org/10.1016/j.commatsci.2019.109197>
6. G.B. McFadden et al., Phase-field models for anisotropic interfaces. *Phys. Rev. E* **48**, 2016–2024 (1993). <https://doi.org/10.1103/PhysRevE.48.2016>
7. H. Salama et al., Role of inclination dependence of grain boundary energy on the microstructure evolution during grain growth. *Acta Mater.* **188**, 641–651 (2020). <https://doi.org/10.1016/j.actamat.2020.02.043>
8. I. Steinbach, X. Song, A. Hartmaier, Phase-field model with plastic flow for grain growth in nanocrystalline material. *Philos. Mag.* **90** (2010). <https://doi.org/10.1080/14786430903074763>
9. A.A. Wheeler, Cahn–Hoffman ξ -vector and its relation to diffuse interface models of phase transitions. *J. Stat. Phys.* **95**, 1245–1280 (1999)
10. G. Wulff, On the question of speed of growth and dissolution of crystal surfaces. *Z. Krist.* **34**(5/6), 449 (1901)

Open Access This chapter is licensed under the terms of the Creative Commons Attribution 4.0 International License (<http://creativecommons.org/licenses/by/4.0/>), which permits use, sharing, adaptation, distribution and reproduction in any medium or format, as long as you give appropriate credit to the original author(s) and the source, provide a link to the Creative Commons license and indicate if changes were made.

The images or other third party material in this chapter are included in the chapter’s Creative Commons license, unless indicated otherwise in a credit line to the material. If material is not included in the chapter’s Creative Commons license and your intended use is not permitted by statutory regulation or exceeds the permitted use, you will need to obtain permission directly from the copyright holder.

